Letters

Saturated *dq*-Axis Inductance Offline Identification Method for SynRM Based on a Novel Active Flux Observer Orientation

Tong Jin, Wei Sun, *Member, IEEE*, Haowen Wang, Dong Jiang, *Senior Member, IEEE*, and Ronghai Qu, *Fellow, IEEE*

***Abstract*—The precision of motor parameters directly affects the control performance of SynRMs drive system. Currently, high-frequency injection methods often generate noise and are unsuitable for high-power and low carrier wave ratio scenarios. Meanwhile, model-based methods can only identify the saturation characteristics of the L_d without calibration bench loading. This letter proposes an identification method based on a novel active flux observer orientation, which does not require high-frequency injection or calibration bench loading to identify the saturation characteristics of *dq*-axis inductance. During identification L_d, the active flux observer adopts *d*-axis orientation and identifies the saturation values of L_d by applying different i_d. When identifying the L_q, the active flux observer adopts negative *q*-axis orientation, and the output of the speed loop is used as the input for the *d*-axis current loop. By applying different i_q, the saturation values of L_q are identified. Experimental results show the validity of the proposed method.**

***Index Terms*—Active flux observer, parameter identification, rotating state, synchronous reluctance motor.**

I. Introduction

DUE to the scarcity of rare Earth resources, synchronous reluctance motors have garnered widespread attention in industrial systems in recent years, owing to their advantages of being devoid of permanent magnets and possessing a simple structure [1], [2], [3].

Due to the serious saturation effect of synchronous reluctance motors, the inductance parameters of SynRMs exhibit significant variations at no-load and full-load conditions. The saturation characteristics of inductance have a considerable impact on sensorless control algorithms based on motor mathematical models [4], [5], [6]. To achieve excellent control performance of sensorless algorithms for synchronous reluctance motors, it is necessary to identify inductance parameters considering saturation effects.

Manuscript received 6 March 2024; revised 14 April 2024; accepted 30 April 2024. Date of publication 13 May 2024; date of current version 16 July 2024. This work was supported by the National Natural Science Foundation of China under Grant 52122705. *(Corresponding author: Wei Sun.)*

The authors are with the School of Electrical and Electronic Engineering, Huazhong University of Science and Technology, Wuhan 430074, China (e-mail: jintong@hust.edu.cn; sunwei77@hust.edu.cn; m202171935@hust.edu.cn; jiangd@hust.edu.cn; ronghaiqu@hust.edu.cn).

Color versions of one or more figures in this article are available at https://doi.org/10.1109/TPEL.2024.3400125.

Digital Object Identifier 10.1109/TPEL.2024.3400125

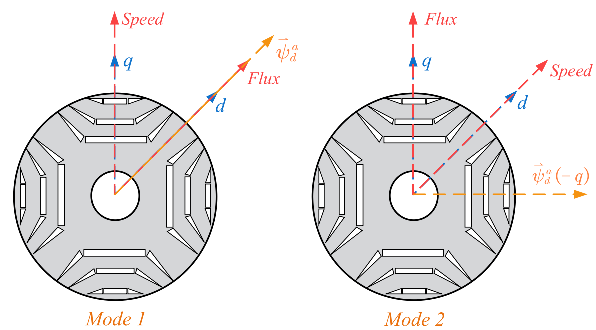

Fig. 1. Schematic diagram of the relative positions of the *flux–speed* axis, *d-q* axis, and $\vec{\psi}_d^a$ in two scenarios.

The existing identification methods mainly include high-frequency injection-based methods, model-based methods, and methods for online identification. In [7], [8], and [9], the high-frequency injection method is employed for motor parameter identification. However, this approach is somewhat constrained due to its tendency to generate noise and its inapplicability in high-power motor and low carrier wave ratio scenarios. In [10], parameter identification is conducted through the use of a calibration bench loading. But when the motor lacks loading from the calibration bench, model-based offline parameter identification in rotating states can only recognize the saturation characteristics of the *d*-axis inductance, while unable to identify the saturation characteristics of the *q*-axis inductance. In [11] and [12], motor parameter calibration is conducted using a calibration bench. Nevertheless, this method also necessitates loading from the calibration bench and requires the collection of extensive data, making its operational procedure quite complex. In [13] and [14], a method is mentioned that converts the circuit of permanent magnet synchronous motors (PMSMs) into a series circuit of resistance and inductance and identifies the inductance parameters by injecting a step voltage signal and solving the first-order differential equation response. This method can identify the saturation characteristics of the inductance when the motor is in a static state. In [15], [16], and [17], binary function models for inductance concerning *dq*-axis currents are both proposed, with parameter identification conducted through genetic algorithms. Undoubtedly, this approach significantly increases the complexity and cost associated with identification.

Different from traditional identification methods that rely on either calibration benches or high-frequency injection, as well as online identification, this letter proposes an offline identification method for inductance in rotating states based on active flux observer. This method employs a new active flux observer orientation mode to address the inability to identify the saturation characteristics of the *q*-axis inductance due to the absence of loading on the calibration bench. Finally, the proposed method is validated through experiments.

The main contribution of this letter lies in the offline identification of saturation characteristic curves of inductance without the need for high-frequency injection or calibration benches.

II. Two Different Orientation Methods for Active Flux Observer

The relevant content of the active flux observer is referenced in [18]. In contrast to the traditional orientation method of the active flux observer, this letter proposes a new orientation method. The specific description is as follows.

The torque equation of the SynRM can be expressed as shown in the following:

$$T_e = \frac{3}{2} n_p (L_d - L_q) i_d i_q. \quad (1)$$

The introduction of field-oriented control in motor control aims to decouple the *dq* currents, thereby enabling one current to control torque while the other current controls flux. In traditional control methods, the *d*-axis current controls the flux while the *q*-axis current controls the torque. However, for SynRM with torque equations, as shown in (1), this control rule can be reversed (i.e., the *d*-axis current controls the torque while the *q*-axis current controls the flux).

The rotor of a SynRM is typically oriented such that the direction with no magnetic barrier in the physical structure is chosen as the *d*-axis direction, while the axis with a leading *d*-axis electrical angle of 90° is defined as the *q*-axis direction. However, the stator axis system does not have any practical physical significance. Departing from the traditional *dq*-axis definition for the stator, the two command currents of the current loop are defined as *flux* and *speed*, where *flux* represents the given current value and *speed* represents the output value of the speed loop PI controller. Thus, the stator axis system is defined as the *flux–speed* axis, while the rotor axis system is defined as the *d-q* axis. In the unloaded state of the SynRM, there are only two possible relative positions between the stator *flux–speed* axis and the rotor *d-q* axis, as illustrated in Fig. 1.

The formula for the $\vec{\psi}_d^a$ of traditional SynRM has been improved to obtain (2), and the new active flux observer orientation method proposed in this paper is based on this equation

$$\begin{aligned} \vec{\psi}_d^a &= \vec{\psi}_s - L_x \vec{i}_s \\ &= (\psi_d + j\psi_q) - L_x(i_d + j i_q) \\ &= (\psi_d - L_x i_d) + j(\psi_q - L_x i_q) \\ &= (L_d i_d - L_x i_d) + j(L_q i_q - L_x i_q) \\ &= (L_d - L_x) i_d + j(L_q - L_x) i_q \end{aligned} \quad (2)$$

where $x = d, q$.

A. Mode 1: Traditional d-Axis Orientation Method

When $x = q$ in (2), $\vec{\psi}_d^a = (L_d - L_q) i_d$, indicating that $\vec{\psi}_d^a$ is oriented along the *d*-axis, as shown in *Mode 1* of Fig. 1. To achieve $\vec{\psi}_d^a$ orientation, i_d cannot be zero; otherwise, $\vec{\psi}_d^a$ would be a zero vector and cannot be oriented. However, since the motor is in a no-load condition, according to the (1), i_q must be zero. In this case, the observed angle of the active flux observer can be directly used as the feedback angle for coordinate transformation. The output of the speed loop serves as the input to the *q*-axis current loop, while the given current is i_d. As the given value i_d is not zero, the active flux observer can perform closed-loop control normally. In this scenario, by specifying different values of i_d, the saturation characteristics of the *d*-axis inductance under different i_d can be identified.

B. Mode 2: The Proposed Negative q-Axis Orientation Method

When $x = d$ in (2), $\vec{\psi}_d^a = -j(L_d - L_q) i_q$, indicating that $\vec{\psi}_d^a$ is oriented along the negative *q*-axis, as shown in *Mode 2* of Fig. 1. Similarly, in this case, i_q must not be zero, and i_d must be zero. In this scenario, the observed angle of the active flux observer needs to be increased by $\pi/2$ to serve as the feedback angle for coordinate transformation. Another difference from *Mode 1* is that in this case, the output of the speed loop serves as the input to the *d*-axis current loop, while the given current is i_q. As explained earlier, this situation is both existent and reasonable. Similarly, by specifying different values of i_q, the saturation characteristics of the *q*-axis inductance can be identified.

III. Proposed Offline Parameter Identification Method

A. SynRM Model for Parameter Identification

The proposed offline parameter identification method is based on the *dq*-axis voltage equation of synchronous reluctance motors

$$\begin{cases} u_d = R_s i_d + L_d \frac{di_d}{dt} - \omega_e L_q i_q \\ u_q = R_s i_q + L_q \frac{di_q}{dt} + \omega_e L_d i_d \end{cases} \quad (3)$$

where ω_e is the electrical angular velocity, i_d is the *d*-axis current, i_q is the *q*-axis current, u_d is the *d*-axis voltage, u_q is the *q*-axis voltage, R_s is the stator resistance, L_d is the *d*-axis inductance, and L_q is the *q*-axis inductance.

B. d-Axis Inductance Identification

The vector control scheme employing dual closed-loops for speed and current is utilized, and the angle information of the rotor is the observation angle of the active flux observer in *Mode 1*. The *d*-axis current i_{d_ref} command is initiated at 30% of the rated current magnitude and is increased by 10% every 2 s until reaching the rated current magnitude. The reason for starting from $30\% I_N$ is that the saturation phenomenon of the inductance is not significant at currents below 30% of the rated current. Therefore, we chose the current range of 30%–$100\% I_N$ for the identification interval. The speed reference ω_{e_ref} is set to 40% of the rated speed. The control block diagram is shown

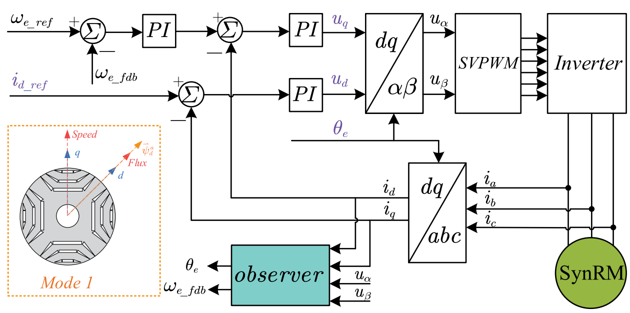

Fig. 2. Control Block Diagram for Identifying L_d (*Mode 1*).

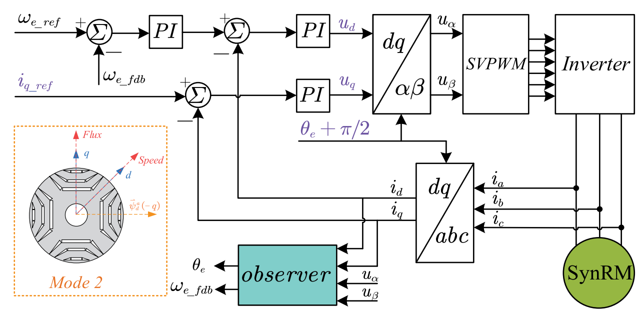

Fig. 3. Control Block Diagram for Identifying L_q (*Mode 2*).

in Fig. 2, where ω_{e_fdb} is the estimated speed of the observer, θ_e is the estimated electrical angle of the observer, u_α is the α-axis voltage, and u_β is the β-axis voltage.

When the motor operates at steady state, the derivative of the current is zero. From (3), the calculation formula for the d-axis inductance can be derived as follows:

$$L_d = \frac{u_q - R_s i_q}{\omega_e i_d}. \tag{4}$$

The saturation characteristic curve of L_d under the entire operating condition is fitted using a fourth-degree polynomial to the eight points identified from the aforementioned steps. It is assumed that the d-axis inductance remains unsaturated when $i_{d\_\text{ref}} \leq 30\% I_N$, meaning the d-axis inductance remains constant at the value identified when $i_{d\_\text{ref}} = 30\% I_N$. Therefore, the fitted saturation characteristic curve equation is represented as follows:

$$\begin{cases} L_d = L_{d1}, 0 \leqslant i_d \leqslant 30\% I_N \\ L_d = a_1 i_d^4 + b_1 i_d^3 + c_1 i_d^2 + d_1 i_d + e_1, 30\% I_N \leqslant i_d \leqslant I_N \end{cases} \tag{5}$$

where L_{d1} represents the value of the d-axis inductance when it is not in saturation state; a_1, b_1, c_1, d_1, and e_1 are undetermined coefficients of the fitting curve, which can be determined using the least squares fitting method; I_N represents the rated current.

q-axis inductance identification: Due to the unique rotor structure of synchronous reluctance motors, regardless of whether the d-axis or q-axis current vector is given, the magnetic flux always follows the path of least reluctance (i.e., the d-axis of the SynRM). Consequently, the rotor orientation always aligns with the d-axis. In this scenario, for the motor in a no-load state, the d-axis current is nonzero, implying that the q-axis current must be zero, making it impossible to identify the q-axis inductance parameters.

Based on the active flux observer orientation proposed in this letter (i.e., Mode 2), the negative q-axis mode takes the output command of the speed loop as the input command of the d-axis current loop, and the q-axis current reference i_{q_ref} command is initiated at 30% of the rated current magnitude, with the speed outer loop set at 40% of the rated speed. Every 2 s, the i_{q_ref} command is increased by 10% until reaching the rated current magnitude. This procedure enables the saturation characteristics of L_q to be obtained at different i_q values by controlling the magnitude of i_q. The control block diagram is shown in Fig. 3.

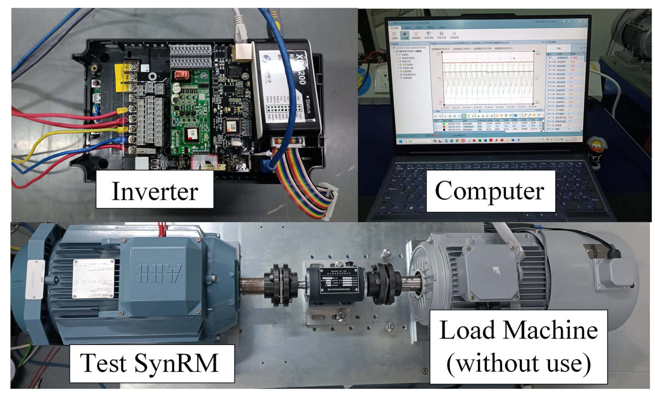

Fig. 4. 5.5-KW SynRM drive experimental platform.

TABLE I
SynRM Parameters

Parameter	Value	Parameter	Value
Rated Power	5.5 KW	Rated Torque	35 N·m
Rated Speed	1500 r/min	Resistance	0.56643 Ω
Rated Frequency	50 Hz	*d*-axis inductance	128.15 mH
Rated Current	12.1 A	*q*-axis inductance	23.60 mH
Rated Voltage	380 V	Number of Pole Paris	2

When the motor operates at steady state, the derivative of the current is zero. From (3), the calculation formula for the q-axis inductance can be derived as follows:

$$L_q = \frac{u_d - R_s i_d}{-\omega_e i_q}. \tag{6}$$

Similarly, fit a saturation characteristic curve of L_q using the aforementioned method of fitting L_d.

IV. Experimental Result

The method proposed in this letter is validated on the experimental platform shown in Fig. 4. The motor is a pure reluctance synchronous reluctance motor from ABB, with specific parameters detailed in Table I.

The identification results for L_d and L_q using the method proposed in this letter are shown in Figs. 5 and 6, respectively. In both cases, the current changes in intervals of 10% of the rated current, from 30% to 100% of the rated current, while the speed is maintained at 40% of the rated speed. The experimental

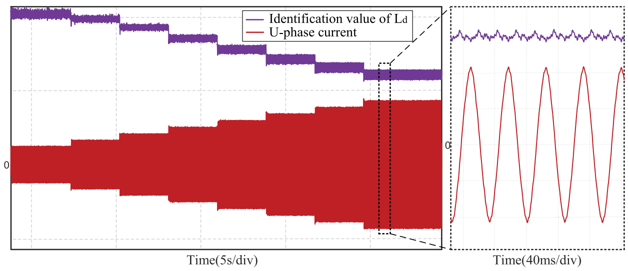

Fig. 5. Experimental results of offline identification of d-axis inductance using the proposed method.

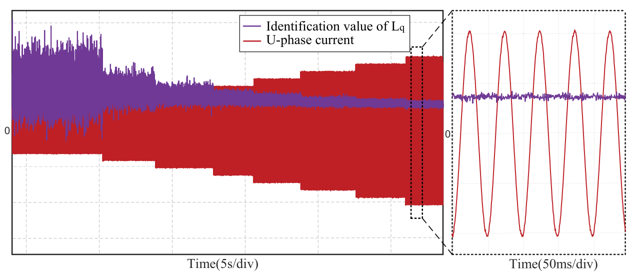

Fig. 6. Experimental results of offline identification of q-axis inductance using the proposed method.

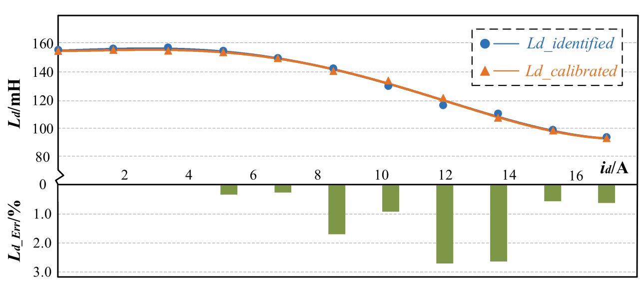

Fig. 7. Identification and calibration of d-axis inductance saturation characteristic curve.

results show that the dq-axis inductances exhibit varying degrees of saturation due to different currents.

Taking Fig. 5 as an example. Because the denominator in the voltage equation identification process cannot be zero, and the motor starts slower when the current is too low, the minimum set current is defined as 30% of the rated current. Furthermore, the saturation effect of the SynRMs is minimal at low currents, leading to the assumption that the change in inductance parameters at low currents is negligible.

Therefore, based on the identified eight values of inductance, the inductance values at $i_d = 0, 10\%I_N, 20\%I_N$ are artificially set to the value identified at $i_d = 30\%I_N$. This approach results in 11 d-axis inductance values. The saturation characteristic curve fitted from these 11 values using a fourth-degree polynomial is shown in Fig. 7. Fig. 7 reveals that under the condition of $i_q = 0$, L_d decreases as i_d increases due to magnetic saturation.

Similarly, Fig. 6 shows the identified eight values of L_q. Fig. 8 shows the saturation characteristic curve fitted for L_q. From Fig. 8, it can be observed that under the condition of $i_d = 0$, as i_q increases, L_q decreases due to magnetic saturation.

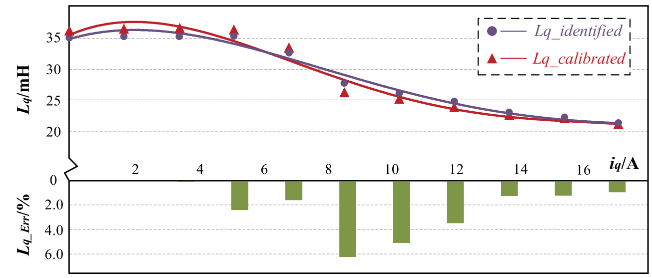

Fig. 8. Identification and calibration of q-axis inductance saturation characteristic curve.

TABLE II
IDENTIFICATION AND CALIBRATION VALUES OF DQ-AXIS INDUCTANCE AND THEIR ERRORS

i_{dq_ref}/A	5.13	6.84	8.56	10.27	11.98	13.69	15.40	17.11
L_{d_ide}/mH	155.58	150.33	142.52	131.74	116.55	110.37	99.08	92.12
L_{d_cal}/mH	155.08	149.96	140.15	132.95	119.78	107.54	98.53	92.68
L_{d_err}/%	0.32	0.25	1.69	0.91	2.70	2.63	0.55	0.61
L_{q_ide}/mH	35.23	32.64	27.83	26.23	24.83	23.18	22.38	21.26
L_{q_cal}/mH	36.07	33.14	26.22	24.98	24.01	22.91	22.13	21.07
L_{q_err}/%	2.32	1.51	6.15	5.00	3.40	1.17	1.15	0.88

The motor inductance is calibrated using a test bench. The calibration method involves operating the "Drag Motor" in speed mode and the "Test SynRM" in torque mode. By providing different dq-axis currents to the "Test SynRM", the corresponding dq-axis inductances under various saturation levels are obtained. The calibrated inductance corresponding to saturation levels similar to those in the identification conditions is then selected as a reference. (Although the cross saturation effect has a certain impact on motor parameters under light load, the control accuracy under light load is minimally affected by parameter errors). The calibrated values of L_d and L_q are listed in Table II. Comparing the identification results with the calibration results, the average identification error for L_d is 1.21%, with a maximum error of 2.70%. The average identification error for L_q is 2.69%, with a maximum error of 6.15%. In addition, the dq-axis inductances of the "Test SynRM" obtained through the self-learning function of a General-Purpose Inverter from ABB are $L_d = 125.54$ mH and $L_q = 23.45$ mH. It is evident that the self-learning function can only obtain the inductance values under specific saturation levels and cannot obtain the saturation characteristic curve of the inductance.

V. CONCLUSION

This letter proposes a novel offline parameter identification method based on two different orientation modes of the active flux observer. By orienting the vector $\vec{\psi}_d^a$ in the negative q-axis direction, the method resolves the problem of traditional methods being unable to identify the q-axis inductance saturation characteristics of SynRMs. Compared to traditional methods, this approach fully considers the effects of magnetic saturation and accurately identifies the dq-axis inductance and its saturation characteristics without the need for position sensors or calibration benches. Furthermore, the identification strategy has discarded the high-frequency injection method, which is not suitable for high-power and low carrier wave ratio scenarios.

The saturation characteristics curve identified by the proposed method can be utilized for the design of position sensorless control systems.

References

[1] M. Murataliyev, M. Degano, M. Di Nardo, N. Bianchi, and C. Gerada, "Synchronous reluctance machines: A comprehensive review and technology comparison," *Proc. IEEE*, vol. 110, no. 3, pp. 382–399, Mar. 2022, doi: 10.1109/JPROC.2022.3145662.

[2] A. Vagati, M. Pastorelli, and G. Franceschini, "High-performance control of synchronous reluctance motors," *IEEE Trans. Ind. Appl.*, vol. 33, no. 4, pp. 983–991, Jul./Aug. 1997, doi: 10.1109/28.605740.

[3] H. Heidari et al., "A review of synchronous reluctance motor-drive advancements," *Sustainability*, vol. 13, no. 2, 2021, Art. no. 729.

[4] S. Morimoto, M. Sanada, and Y. Takeda, "Mechanical sensorless drives of IPMSM with online parameter identification," *IEEE Trans. Ind. Appl.*, vol. 42, no. 5, pp. 1241–1248, Sep./Oct. 2006, doi: 10.1109/TIA.2006.880840.

[5] M. Hinkkanen, P. Pescetto, E. Mölsä, S. E. Saarakkala, G. Pellegrino, and R. Bojoi, "Sensorless self-commissioning of synchronous reluctance motors at standstill without rotor locking," *IEEE Trans. Ind. Appl.*, vol. 53, no. 3, pp. 2120–2129, May/Jun. 2017, doi: 10.1109/TIA.2016.2644624.

[6] Shinji Ichikawa et al., "Sensorless control of synchronous reluctance motors based on extended electromotive force model and inductance measurement," *Elect. Eng. Jpn.*, vol. 160, no. 4, pp. 70–80, 2010.

[7] K. Yu and Z. Wang, "Online decoupled multi-parameter identification of dual three-phase IPMSM under position-offset and HF signal injection," *IEEE Trans. Ind. Electron.*, vol. 71, no. 4, pp. 3429–3440, Apr. 2024, doi: 10.1109/TIE.2023.3273256.

[8] Q. Wang et al., "An offline parameter self-learning method considering inverter nonlinearity with zero-axis voltage," *IEEE Trans. Power Electron.*, vol. 36, no. 12, pp. 14098–14109, Dec. 2021.

[9] S. Liu et al., "Virtual-axis injection based online parameter identification of PMSM considering cross coupling and saturation effects," *IEEE Trans. Power Electron.*, vol. 38, no. 5, pp. 5791–5802, May 2023.

[10] B. Stumberger, B. Kreca, and B. Hribernik, "Determination of parameters of synchronous motor with permanent magnets from measurement of load conditions," *IEEE Trans. Energy Convers.*, vol. 14, no. 4, pp. 1413–1416, Dec. 1999, doi: 10.1109/60.815082.

[11] G. Pellegrino, B. Boazzo, and T. M. Jahns, "Magnetic model self-identification for PM synchronous machine drives," *IEEE Trans. Ind. Appl.*, vol. 51, no. 3, pp. 2246–2254, May/Jun. 2015.

[12] M. Cao, J. Egashira, and K. Kaneko, "High efficiency control of IPMSM for electric motorcycles," in *Proc. IEEE 6th Int. Power Electron. Motion Control Conf.*, 2009, pp. 1893–1897, doi: 10.1109/IPEMC.2009.5157705.

[13] D. Pengcheng, X. Dianguo, W. Bo, and Y. Yong, "Offline parameter identification strategy of permanent magnet synchronous motor considering the inverter nonlinearities," in *Proc. 25th Int. Conf. Elect. Machines Syst.*, 2022, pp. 1–5, doi: 10.1109/ICEMS56177.2022.9983312.

[14] Q. Wang, G. Zhang, G. Wang, C. Li, and D. Xu, "Offline parameter self-learning method for general-purpose PMSM drives with estimation error compensation," *IEEE Trans. Power Electron.*, vol. 34, no. 11, pp. 11103–11115, Nov. 2019, doi: 10.1109/TPEL.2019.2900559.

[15] T. -G. Woo, S. -W. Park, S. -C. Choi, H. -J. Lee, and Y. -D. Yoon, "Flux saturation model including cross saturation for synchronous reluctance machines and its identification method at standstill," *IEEE Trans. Ind. Electron.*, vol. 70, no. 3, pp. 2318–2328, Mar. 2023, doi: 10.1109/TIE.2022.3174233.

[16] A. Accetta, M. Cirrincione, M. Pucci, and A. Sferlazza, "A saturation model of the synchronous reluctance motor and its identification by genetic algorithms," in *Proc. IEEE Energy Convers. Congr. Expo.*, 2018, pp. 4460–4465, doi: 10.1109/ECCE.2018.8558250.

[17] A. Accetta, M. Cirrincione, M. C. Di Piazza, G. La Tona, M. Luna, and M. Pucci, "Analytical formulation of a maximum torque per ampere (MTPA) technique for SynRMs considering the magnetic saturation," in *Proc. IEEE Energy Convers. Congr. Expo.*, 2019, pp. 4024–4029, doi: 10.1109/ECCE.2019.8912653.

[18] I. Boldea, M. C. Paicu, and G. -D. Andreescu, "Active flux concept for motion-sensorless unified AC drives," *IEEE Trans. Power Electron.*, vol. 23, no. 5, pp. 2612–2618, Sep. 2008.